

Alma Mater Studiorum Università di Bologna  
Archivio istituzionale della ricerca

Empirical Characterization of Track Dimensions for CMT-Based WAAM Processes

This is the final peer-reviewed author's accepted manuscript (postprint) of the following publication:

*Published Version:*

Lettori, J., Raffaeli, R., Bilancia, P., Borsato, M., Peruzzini, M., Pellicciari, M. (2024). Empirical Characterization of Track Dimensions for CMT-Based WAAM Processes. N.A. : Springer Nature AG [10.1007/978-3-031-38241-3\_47].

*Availability:*

This version is available at: <https://hdl.handle.net/11585/964164> since: 2024-02-29

*Published:*

DOI: [http://doi.org/10.1007/978-3-031-38241-3\\_47](http://doi.org/10.1007/978-3-031-38241-3_47)

*Terms of use:*

Some rights reserved. The terms and conditions for the reuse of this version of the manuscript are specified in the publishing policy. For all terms of use and more information see the publisher's website.

This item was downloaded from IRIS Università di Bologna (<https://cris.unibo.it/>).  
When citing, please refer to the published version.

(Article begins on next page)

# Metadata of the chapter that will be visualized in SpringerLink

Book Title	Flexible Automation and Intelligent Manufacturing: Establishing Bridges for More Sustainable Manufacturing Systems	
Series Title		
Chapter Title	Empirical Characterization of Track Dimensions for CMT-Based WAAM Processes	
Copyright Year	2024	
Copyright HolderName	The Author(s), under exclusive license to Springer Nature Switzerland AG	
Corresponding Author	Family Name	<b>Lettori</b>
	Particle	
	Given Name	<b>Jacopo</b>
	Prefix	
	Suffix	
	Role	
	Division	Department of Engineering “Enzo Ferrari”
	Organization	University of Modena and Reggio Emilia
	Address	Modena, Italy
	Division	
	Organization	Universidade Tecnológica Federal do Paraná
	Address	Campus Curitiba, Paraná, Brazil
	Email	jacopo.lettori@unimore.it
	ORCID	<a href="http://orcid.org/0000-0002-8523-8469">http://orcid.org/0000-0002-8523-8469</a>
Author	Family Name	<b>Raffaeli</b>
	Particle	
	Given Name	<b>Roberto</b>
	Prefix	
	Suffix	
	Role	
	Division	Department of Sciences and Methods for Engineering
	Organization	University of Modena and Reggio Emilia
	Address	Modena, Italy
	Email	
	ORCID	<a href="http://orcid.org/0000-0003-0301-454X">http://orcid.org/0000-0003-0301-454X</a>
Author	Family Name	<b>Bilancia</b>
	Particle	
	Given Name	<b>Pietro</b>
	Prefix	
	Suffix	
	Role	
	Division	Department of Sciences and Methods for Engineering
	Organization	University of Modena and Reggio Emilia
	Address	Modena, Italy
	Email	

	ORCID	<a href="http://orcid.org/0000-0002-4931-1745">http://orcid.org/0000-0002-4931-1745</a>
Author	Family Name	<b>Borsato</b>
	Particle	
	Given Name	<b>Milton</b>
	Prefix	
	Suffix	
	Role	
	Division	
	Organization	Universidade Tecnológica Federal do Paraná
	Address	Campus Curitiba, Paraná, Brazil
	Email	
	ORCID	<a href="http://orcid.org/0000-0002-3607-8315">http://orcid.org/0000-0002-3607-8315</a>
Author	Family Name	<b>Peruzzini</b>
	Particle	
	Given Name	<b>Margherita</b>
	Prefix	
	Suffix	
	Role	
	Division	Department of Engineering “Enzo Ferrari”
	Organization	University of Modena and Reggio Emilia
	Address	Modena, Italy
	Email	
	ORCID	<a href="http://orcid.org/0000-0003-2260-0392">http://orcid.org/0000-0003-2260-0392</a>
Author	Family Name	<b>Pellicciari</b>
	Particle	
	Given Name	<b>Marcello</b>
	Prefix	
	Suffix	
	Role	
	Division	Department of Sciences and Methods for Engineering
	Organization	University of Modena and Reggio Emilia
	Address	Modena, Italy
	Email	
	ORCID	<a href="http://orcid.org/0000-0003-2578-4123">http://orcid.org/0000-0003-2578-4123</a>

Abstract Wire Arc Additive Manufacturing is based on a welding torch usually attached to a robotic arm with multiple degrees of freedom. Robot-based additive manufacturing allows non-planar and non-uniform thickness layers to be deposited where the slices have non-constant thickness. Thus, in addition to the motion settings, fine regulations of the welding parameters become necessary to obtain variable bead heights in the same slice. This paper aims to evaluate the user-accessible welding parameters’ influence on the deposited material’s dimensions during continuous Cold Metal Transfer (CMT) and its variant named CMT Cycle Step. In particular, the height and width of beads are investigated by varying the travel speed and the wire-feed rate (continuous CMT), as well as the size of the droplets by varying the number of CMT cycles and the wire-feed rate (CMT Cycle Step). In particular, the characterization of the material deposited during the CMT Cycle Step is not deeply studied in the literature. The experimental specimens are measured and the obtained values are numerically processed to yield empirical formulas that link the dimensions of the deposited material with the selected process parameters. The results show that CMT Cycle Step is more stable than continuous CMT, which confirms its higher suitability for accurate manufacturing.







Keywords  
(separated by '-')

Wire and Arc Additive Manufacturing - Bead Modeling - Cold Metal Transfer - Experimental  
characterization

---



# Empirical Characterization of Track Dimensions for CMT-Based WAAM Processes

Jacopo Lettori<sup>1,2</sup> , Roberto Raffaeli<sup>3</sup> , Pietro Bilancia<sup>3</sup> , Milton Borsato<sup>2</sup> ,  
Margherita Peruzzini<sup>1</sup> , and Marcello Pellicciari<sup>3</sup> 

<sup>1</sup> Department of Engineering “Enzo Ferrari”, University of Modena and Reggio Emilia, Modena, Italy

[jacopo.lettori@unimore.it](mailto:jacopo.lettori@unimore.it)

<sup>2</sup> Universidade Tecnológica Federal do Paraná, Campus Curitiba, Paraná, Brazil

<sup>3</sup> Department of Sciences and Methods for Engineering, University of Modena and Reggio Emilia, Modena, Italy

[AQ1](#)

**Abstract.** Wire Arc Additive Manufacturing is based on a welding torch usually attached to a robotic arm with multiple degrees of freedom. Robot-based additive manufacturing allows non-planar and non-uniform thickness layers to be deposited where the slices have non-constant thickness. Thus, in addition to the motion settings, fine regulations of the welding parameters become necessary to obtain variable bead heights in the same slice. This paper aims to evaluate the user-accessible welding parameters’ influence on the deposited material’s dimensions during continuous Cold Metal Transfer (CMT) and its variant named CMT Cycle Step. In particular, the height and width of beads are investigated by varying the travel speed and the wire-feed rate (continuous CMT), as well as the size of the droplets by varying the number of CMT cycles and the wire-feed rate (CMT Cycle Step). In particular, the characterization of the material deposited during the CMT Cycle Step is not deeply studied in the literature. The experimental specimens are measured and the obtained values are numerically processed to yield empirical formulas that link the dimensions of the deposited material with the selected process parameters. The results show that CMT Cycle Step is more stable than continuous CMT, which confirms its higher suitability for accurate manufacturing.

[AQ2](#)

[AQ3](#)

**Keywords:** Wire and Arc Additive Manufacturing · Bead Modeling · Cold Metal Transfer · Experimental characterization

## 1 Introduction

Robot-Based Additive Manufacturing (RBAM) is the combination of robotic solutions and additive manufacturing technologies. For instance, Wire Arc Additive Manufacturing (WAAM) is a metal wire additive deposition method consisting of an automatized welding process where parts are realized thanks to a torch attached to a manipulator [1]. Usually, WAAM is based on metal-arc inert/active welding techniques [2]. Nowadays, many WAAM processes are based on Cold Metal Transfer (CMT) inert gas welding, which provides high control of the material deposition and requires low thermal input

[3]. With CMT, the material can be either deposited continuously to develop a bead (continuous CMT, Fig. 1a) or by controlling the number of individual droplets per welding spot and the pause time between cycles (CMT Cycle Step, Fig. 1b). The CMT Cycle Step can be used in continuous paths to form a bead composed of successively deposited drops. This approach strongly reduces the input thermal energy and the residual stresses. However, the distance among drops affects the overall quality of the final output and can increase the formation of voids and gaps. Also, the CMT Cycle Step can be used in dot-by-dot printing to develop bars/columns (see Fig. 1b). This method is suited to manufacture lattice structures.

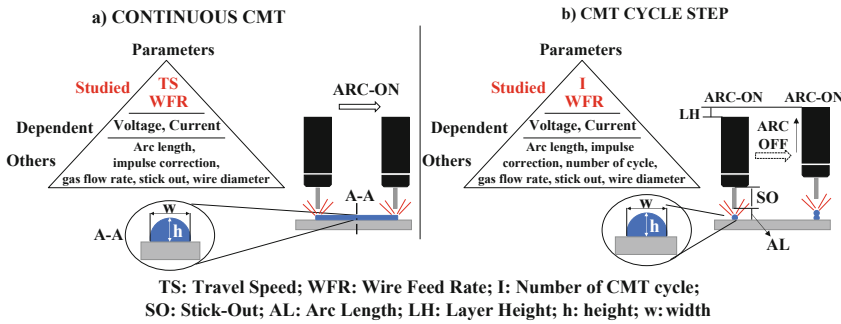


**Fig. 1.** CMT processes and parameters: a) Continuous; b) Cycle Step.

As known, RBAM increases the manufacturing flexibility of cartesian 3D printers as it enables multiaxial deposition, non-planar and non-uniform thickness layers thanks to the extended motion capabilities [2]. Nevertheless, in addition to the higher number of motion parameters to be controlled, one must also consider that the dimensions of the deposited material (i.e., height  $h$  and width  $w$  as in Fig. 1) vary according to the process parameters. Figure 1 summarizes all the principal process parameters involved in WAAM. Previous studies have analyzed the effects of such parameters on the bead dimensions. For example, Wire Feed Rate (WFR), Travel Speed (TS), current, and Argon flow rate were studied to analyze the bead geometry and microstructure [4]. Also, TS and WFR were varied to analyze the bead dimension alteration in [5], generating a predictive model based on neural network. Similarly, TS, WFR, arc voltage and stick-out were varied in [6], whereas TS, WFR and peak current were evaluated in [7, 8]. All these studies reported practical response surfaces or predictive models obtained from experimental observations with continuous CMT. Generally, scarce applications of the CMT Cycle Step can be found in the literature. Examples are reported in [9, 10], although these are not focused on the characterization of the droplets dimensions in relation to the process parameters.

Therefore, the goal of this paper is to find the correlation between the expected sizes of the deposited bead/drop and the main process parameters to properly design and control the manufacturing process. The study was conducted for both the CMT processes with a WAAM experimental setup installed on a Delta 3D printer. In the first experiment, WFR and TS were varied in the continuous CMT (Fig. 1a) and  $h$  and  $w$  of

the bead were measured. In the second experiment, WFR and the number of CMT cycles (I) were varied in the CMT Cycle Step. Here, h and w of the droplets were measured.

The experiments were repeated more times and the average results were considered for the elaboration of performance maps (see Table 2 and Table 3.) This study is a crucial part of the framework presented in [11], aimed at defining an end-to-end process for WAAM. The obtained results can be integrated within predictive models to adapt the process parameters according to the imposed bead/droplet dimensions.

## 2 Experiments Setup

The employed equipment is summarized in Table 1 and shown in Fig. 2. The experiments are conducted using a standard Delta 3D printer adopted to move the CMT torch. The results can be extended to other robotic WAAM systems as the study is strictly focused on the welding parameters while no particular motions are imposed during the tests.

**Table 1.** Preliminary setup of the proposed experiments.

3D Printers	DELTA WASP 40 × 70 INDUSTRIAL
Material	Steel ISO 14341-A/G3Si1. Composition: C = 0.09%; Si = 0.82%; Mn = 1.41%; P = 0.011%; S = 0.005%; Cu = 0.023%; Ni = 0.019%; Mo = 0.006%; Cr = 0.25%
Shielding Gas	CORGON 10 (Ar 90% + CO <sub>2</sub> 10%)
Gas flow rate	15 l/min
Welder	Fronius TPS 320i
Torch	CMT
Wire diameter	1.2 mm
Stick Out	10 mm
Arc length	+3
Impulse correction	0

The adopted welder generator is synergic, that is it automatically modulates voltage, current and material thickness (generator parameter) according to the type of material, wire diameter, gas flow rate and WFR via an internal algorithm that affects the printing. Also, it adapts the WFR within a range defined by the manufacturer to maintain constant welding conditions as the stick-out varies. The stick-out is defined as the distance between the end of the nozzle and the position where the wire melts off (see Fig. 1). In the following, the experiments are described.

### 2.1 Continuous CMT Experiment

Table 2 summarizes the process parameters chosen in the continuous CMT experiment. Differently from previous researches, cylindrical deposition paths were selected to reduce residual stresses.

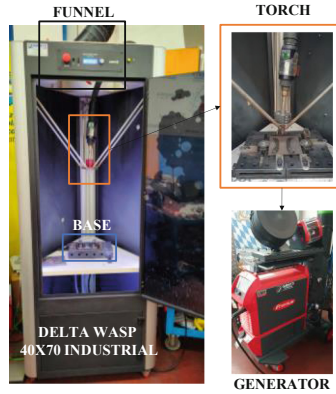


**Fig. 2.** Experimental apparatus.

**Table 2.** Process parameters of continuous CMT. CD x: Centre Distance between two samples in the x direction; CD y: Centre Distance between two samples in the y direction (see Fig. 3).

Parameters	Qualitative analysis		Quantitative analysis
	First part	Second part	\
WFR (m/min)	5, 6, 7	2, 3, 4	1.5, 2, 2.5
TS (mm/s)	15, 17.5, 20	3, 4, 5	3, 4, 5
Layer height (mm)	1.2	1.2	1.2
n° layers	5	5	5
Type of deposition	Spiral	Spiral	Spiral
Substrate [mm]	250 × 150 × 10	250 × 150 × 10	150 × 150 × 8
Sample diameter (mm)	50	50	50
CD x (mm)	65	65	65.15
CD y (mm)	\	70	65.15
n° of experiments	1	1	1
n° samples (i.e. repetitions)	1	2	4
Tot samples (each combination of parameters)	1	2	4

The test consisted of qualitative and quantitative analyses. At first, the qualitative preliminary analysis of the process parameters (WFR and TS) was performed. TS was originally set to a high value (see Table 2), though no satisfactory results were obtained due to the high energy input in a small area. Indeed, samples showed a high waviness both for h and w. After decreasing TS, more stable conditions were reached. Here, the most accurate and stable results were achieved with WFR = 2 m/min for all TS. Some experimental specimens are reported in Fig. 3a and b.



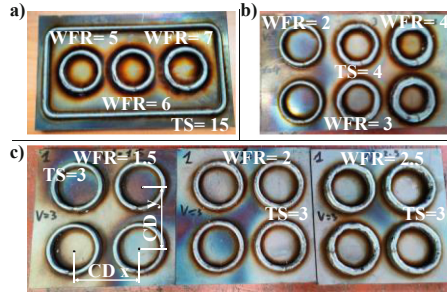


**Fig. 3.** Samples of the continuous CMT: a) Qualitative analysis outputs with high TS; b) Qualitative analysis outputs with low TS; c) Quantitative analysis outputs. Samples measures: CD x (or y): Centre Distance between two samples in the x (or y) direction.

In the second part of the experiment, a quantitative analysis was performed aimed at characterizing the bead  $h$  and  $w$ . In particular, all the possible combinations of WFR and TS were tested (Table 2). Examples of the processed samples are reported in Fig. 3c, whereas numerical result will be discussed in Sect. 3.

## 2.2 CMT Cycle Step Experiment

In a CMT Cycle Step process the material is deposited in a series of digitally controlled welding cycles where droplets are produced. Therefore, column-shaped structures have been manufactured to evaluate the average dimensions of drops ( $h$  and  $w$ ). Table 3 summarizes the considered process parameters, whereas Fig. 4 depicts obtained samples. Each set of columns related to a specific parameter set has been produced separately (i.e., horizontal groups in Fig. 4a). One drop at a time was deposited for each column to ensure a certain cooling time between consecutive depositions.

**Table 3.** Process parameters CMT Cycle Step.

Parameters	Quantitative analysis
WFR (m/min)	2, 2.5, 3, 3.5
I	20, 30, 40, 50
Layer height (mm)	1.2
n° of drops	11
Type of deposition	Cycle Step
n° of cycle	1
Substrate [mm]	150 × 150 × 8
n° of repetitions	3
n° of samples (i.e. repetitions)	4
Tot samples (each combination of parameters)	12

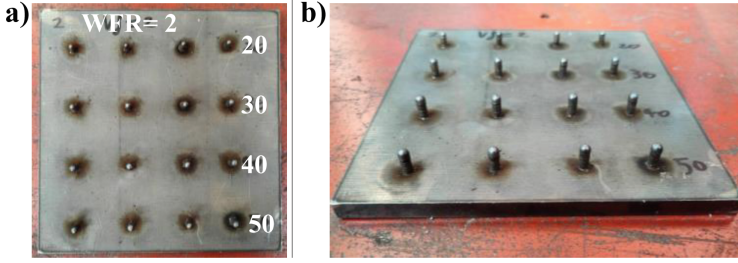


**Fig. 4.** Samples of CMT Cycle Step experiment.

### 3 Results and Discussion

A digital caliper with a resolution of 0.01 mm was adopted to measure the bead sizes and Matlab was used to elaborate the data. The dimensions have been processed in form of polynomial interpolating surfaces both for  $h$  and  $w$  by considering WFR and TS (or  $I$ ) as independent parameters. In particular, Eqs. 1 and 2 have been used to calculate the average height ( $h_{av}$ ) and width ( $w_{av}$ ) of the bead or the drop, whereas Eq. 3 is used to calculate the standard deviation ( $\sigma_{h,w}$ ) of the measures.

$$h_{av} = \frac{\sum_{i=1}^N h_i}{N f} \quad (1)$$

$$w_{av} = \frac{\sum_{i=1}^N w_i}{N} \quad (2)$$

$$\sigma_{h,w} = \sqrt{\frac{\sum_{i=1}^N (x_i - x_{av})^2}{N}} \quad (3)$$

where  $h_i$  is the  $i$ -th measured height,  $w_i$  is the  $i$ -th measured width,  $x$  is one of the two analyzed parameters,  $N$  is the number of measures, and  $f$  is the number of layer or the number of deposited drops, for the first and second experiment respectively.

#### 3.1 Results for the Continuous CMT

Four measures were taken for all the samples in different positions both for  $h$  and  $w$ , which corresponds to sixteen measures for each combination of parameters ( $N = 16$  and  $f = 5$ ). Table 4 summarizes the numerical results, whereas Fig. 5 reports the fitting surfaces of  $h_{av}$  and  $w_{av}$ .

As can be seen from Table 5, the two interpolations fit well the data as SSE and RMSE are relatively low. Also, there are high correlations between the input and the output (high R-square and Adj R-sq). Equations 4 and 5 describe the correlation of  $h_{av}$  and  $w_{av}$  respectively with TS and WFS. However, these equations cannot predict well the bead dimensions outside the range of values used in these experiments. As expected,

$h$  is greater when high WFR and TS are set. In this case, a great quantity of material is deposited (high WFR) in a short time which cools down quickly (high TS). Conversely, high WFS and low TS increase  $w$  as the material is deposited over a longer period of time. This will tend to widen the bead.

**Table 4.** Average values and standard deviations of beads (continuous CMT).

TS (mm/s)	WFR (m/min)	$h_{av}$ (mm)	$\sigma_h$ (mm)	$w_{av}$ (mm)	$\sigma_w$ (mm)
3	1.5	1.68	0.14	4.12	0.06
	2	1.69	0.34	5.12	0.15
	2.5	1.73	0.27	6.36	0.32
4	1.5	1.52	0.24	3.46	0.14
	2	1.52	0.12	4.55	0.08
	2.5	1.56	0.20	5.30	0.32
5	1.5	1.39	0.22	3.30	0.08
	2	1.45	0.07	3.98	0.09
	2.5	1.43	0.33	5.07	0.13

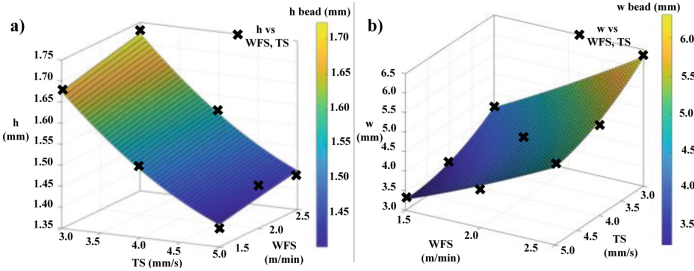


**Fig. 5.** Interpolation surfaces of continuous CMT: a)  $h$ ; b)  $w$ .

Note that, low values of WFR (i.e., 1.5 m/min) can cause printing failures, as shown in Fig. 6. Such failures occur when scarce amount of material is deposited, limiting the ignition of the torch during the execution of the first layer. Hence, a larger WFR should be used during the deposition of the first layers. Once completed, the desired WFR value can then be used.

$$h_{av}(WFR, TS) = 2.395 - 0.3532 TS + 0.07959 WFR + 0.02811 TS^2 - 0.005094 TS WFR - 0.003986 WFR^2 \quad (4)$$

$$w_{av}(WFR, TS) = 5.204 - 1.851 TS + 2.03 WFR + 0.2227 TS^2 - 0.2361 TS WFR + 0.2162 WFR^2 \quad (5)$$

**Table 5.** Fit statistics of continuous CMT. SSE: Sum of Square due to Error; R-square: Coefficient of determination; DFE: Degrees of Freedom; Adj R-sq: Degree-of-freedom adjusted coefficient of determination; RMSE: Root mean squared error (standard error).

	Fit type	SSE	R-square	DFE	Adj R-sq	RMSE
$h_{av}$	Poly22	0.0017	0.9857	3	0.9617	0.0240
$w_{av}$	Poly22	0.0692	0.9910	3	0.9760	0.1519



**Fig. 6.** Printing failure with low WFR.

### 3.2 Results for CMT Cycle Step

One measure was taken for all the samples in different positions both for  $h$  and  $w$  of the drops. That corresponds to twelve measures for each combination of parameters ( $N = 12$  and  $f = 11$ ). Figure 7 reports the fitting surfaces of  $h_{av}$  and  $w_{av}$ , whereas Table 6 summarizes the experiment results. In line with the results presented in Sect. 3.1, also these surfaces fit well the measured data, as can be seen from Table 7. Equations 6 and 7 describe the correlation of  $h$  and  $w$  respectively with  $I$  and WFS. As expected,  $h$  and  $w$  increase with high values of WFR and with high  $I$ . Indeed, WFS determines the deposition rate during the welding process and  $I$  determines the number of CMT cycle for welding spot, thus increasing the size of the droplets.

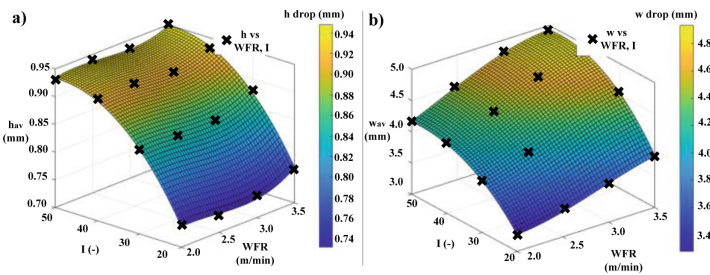


**Fig. 7.** Interpolation surfaces of CMT Cycle Step: a)  $h$ ; b)  $w$ .

$$\begin{aligned}
 h_{av}(WFR, I) = & -0.1209 + 0.5861 WFR + 0.02442 I - 0.2577 WFR^2 \\
 & + 0.003253 WFR I - 0.0003875 I^2 + 0.03697 WFR^3 - 0.0007077 WFR^2 I \\
 & + 5.356e^{-6} WFR I^2 + 1.231e^{-6} I^3
 \end{aligned} \tag{6}$$

**Table 6.** Average values and standard deviations of drops (CMT Cycle Step).

WFR (m/min)	I (-)	$h_{av}$ (mm)	$\sigma_h$ (mm)	$w_{av}$ (mm)	$\sigma_w$ (mm)
2	50	0.93	0.09	4.16	0.03
	40	0.92	0.14	4.13	0.05
	30	0.85	0.10	3.83	0.03
	20	0.74	0.11	3.26	0.05
2.5	50	0.94	0.09	4.48	0.06
	40	0.92	0.11	4.38	0.05
	30	0.85	0.11	4.05	0.03
	20	0.73	0.17	3.44	0.04
3	50	0.93	0.06	4.82	0.08
	40	0.91	0.09	4.70	0.05
	30	0.85	0.09	4.29	0.03
	20	0.74	0.11	3.62	0.06
3.5	50	0.95	0.08	4.91	0.09
	40	0.93	0.09	4.86	0.05
	30	0.88	0.14	4.56	0.06
	20	0.76	0.19	3.82	0.04

**Table 7.** Fit statistics of CMT Cycle Step. SSE: Sum of Square due to Error; R-square: Coefficient of determination; DFE: Degrees of Freedom; Adj R-sq: Degree-of-freedom adjusted coefficient of determination; RMSE: Root mean squared error (standard error).

	Fit type	SSE	R-square	DFE	Adj R-sq	RMSE
$h_{av}$	Poly33	0.00024	0.9975	6	0.9937	0.0063
$w_{av}$	Poly33	0.0072	0.9982	6	0.9954	0.0347

$$\begin{aligned}
 w_{av}(WFR, I) = & 5.859 - 4.846 WFR + 0.04159 I + 1.558 WFR^2 \\
 & + 0.07053 WFR I - 0.001674 I^2 - 0.1587 WFR^3 - 0.008901 WFR^2 I \\
 & - 0.0002433 WFR I^2 + 8.675e^{-6} I^3
 \end{aligned} \quad (7)$$

## 4 Conclusions

This paper presents two experiments aimed at characterizing the dimensions of the deposited material (i.e. bead/drop height and width) in continuous CMT and CMT Cycle Step welding processes. The parameters varied during the experiments are WFR and

TS for the continuous CMT, I and WFR for the CMT Cycle Step. These campaigns are of particular importance for RBAM applications, especially for approaching non-uniform layers and non-planar layers, namely when the slice thickness is not constant and proper tuning operations of process parameters are needed to finely match expected thickness. The tests highlighted that the CMT Cycle Step looks more controllable than continuous CMT, which confirms its higher suitability for accurate manufacturing. As a result of the study, empirical polynomial relations are derived which are valid within the explored design domain and can be utilized during the process design and programming. Similar empirical correlations can potentially be found also with other welding materials, although specific experimental studies become necessary. As a future work, extended experimental campaigns should be conducted by considering higher values of TS and WFR and by analyzing the behavior of multi-beads and multi-droplets overlapping. Finally, a 3D scanner may be used in place of standard measuring tools to acquire the track dimensions and extrapolate accurate datasets.

**Acknowledgment.** The authors wish to acknowledge the Guidetti Technology Srl (Modena, Italy) for their precious collaboration during the experimental work.

## References

1. Jiang, J., Newman, S.T., Zhong, R.Y.: A review of multiple degrees of freedom for additive manufacturing machines. *Int. J. Comput. Integr. Manuf.* **34**(2), 195–211 (2021)
2. Jafari, D., Vaneker, T.H.J., Gibson, I.: Wire and arc additive manufacturing: opportunities and challenges to control the quality and accuracy of manufactured parts. *Mater. Des.* **202**, 109471 (2021)
3. Selvi, S., Vishvakshan, A., Rajasekar, E.: Cold metal transfer (CMT) technology-an overview. *Def. Technol.* **14**(1), 28–44 (2018)
4. Dinovitzer, M., Chen, X., Laliberte, J., Huang, X., Frei, H.: Effect of wire and arc additive manufacturing (WAAM) process parameters on bead geometry and microstructure. *Addit. Manuf.* **26**, 138–146 (2019)
5. Ding, D., Pan, Z., Cuiuri, D., Li, H., Van Duin, S., Larkin, N.: Bead modelling and implementation of adaptive MAT path in wire and arc additive manufacturing. *Robot. Comput. Integr. Manuf.* **39**, 32–42 (2016)
6. Xiong, J., Zhang, G., Hu, J., Wu, L.: Bead geometry prediction for robotic GMAW-based rapid manufacturing through a neural network and a second-order regression analysis. *J. Intell. Manuf.* **25**(1), 157–163 (2012). <https://doi.org/10.1007/s10845-012-0682-1>
7. Panda, B., Shankwar, K., Garg, A., Savalani, M.M.: Evaluation of genetic programming-based models for simulating bead dimensions in wire and arc additive manufacturing. *J. Intell. Manuf.* **30**(2), 809–820 (2016). <https://doi.org/10.1007/s10845-016-1282-2>
8. Geng, H., Xiong, J., Huang, D., Lin, X., Li, J.: A prediction model of layer geometrical size in wire and arc additive manufacture using response surface methodology. *Int. J. Adv. Manuf. Technol.* **93**(1–4), 175–186 (2015). <https://doi.org/10.1007/s00170-015-8147-2>
9. Peng, M., et al.: CMT welding-brazing of Al/steel dissimilar materials using cycle-step mode. *J. Mark. Res.* **18**, 1267–1280 (2022)
10. Votruba, V., et al.: Experimental investigation of CMT discontinuous wire arc additive manufacturing of Inconel 625. *Int. J. Adv. Manuf. Technol.* **122**(2), 711–727 (2022)
11. Lettori, J., Raffaelli, R., Peruzzini, M., Pellicciari, M.: A framework for hybrid manufacturing in robotic cells. *Comput. Aided Des. Appl.* **19**(5), 1029–1041 (2022)

# Author Queries

## Chapter 47

Query Refs.	Details Required	Author's response
AQ1	This is to inform you that corresponding author has been identified as per the information available in the Copyright form.	
AQ2	Per Springer style, both city and country names must be present in the affiliations. Accordingly, we have inserted the city name "Modena" in affiliations "1" and "3". Please check and confirm if the inserted city name is correct. If not, please provide us with the correct city name.	
AQ3	Please check and confirm if the affiliation elements have been correctly identified. Amend if necessary.	